Eur J Vasc Endovasc Surg **26**, 357–366 (2003)
doi: 10.1016/S1078-5884(02)00567-1, available online at http://www.sciencedirect.com on SCIENCE DIRECT®

Correlation of Intimal Hyperplasia Development and Shear Stress Distribution at the Distal End-side-anastomosis, *in vitro* Study Using Particle Image Velocimetry

M. Heise,[1*] U. Krüger,[2] R. Rückert,[3] R. Pfitzman,[1] P. Neuhaus[1] and U. Settmacher[1]

[1]*Charité, Campus Virchow Klinikum, Department of General, Transplantation and Vascular Surgery, Augustenburger Platz 1, 13353 Berlin, Germany,* [2]*Königin Elisabeth Krankenhaus, Department of Vascular Surgery, Herzbergstr. 79, 10365 Berlin, Germany and* [3]*Charité, Campus Mitte, Department of General and Vascular Surgery, Schumannstr. 20/21, 10115 Berlin, Germany*

Low shear areas at the distal anastomosis of peripheral bypasses are thought to promote neointimal hyperplasia. In this study we evaluated the fluid dynamic environment at the distal anastomosis of peripheral bypasses by means of a new method for in vitro *flow visualization and quantitative velocity field measurement.*

A silastic model of a distal end-side anastomosis was attached to a mock circulation loop driven by an artificial heart. High resolution velocity fields were measured by means of particle image velocimetry (PIV). The velocity vector data were used to calculate vorticity ω, strain rates e_x, shear rates h and shear stresses τ. Two separations and a stagnation zone were identified by means of flow visualization. Measured velocities inside the three zones were significantly lower than in the high velocity mainstream. Calculated shear rates and shear stresses inside the zones were significantly lower than human wall shear rates. At the transition between the effective mainstream and the boundary layers high vorticity and compressive strain fields existed, indicating the presence of high shear forces. The locations of these areas corresponded to the well known zones of intimal hyperplasia.

The high resolution shear stress analysis supports the low shear theory of intimal hyperplasia development. A wall diversion angle greater than 6° leads to flow separation and presumed IH promotion until high shear transition areas are reached.

Introduction

The development of anastomotic fibro-intimal hyperplasia (IH) represents one of the main reasons for intermediate and late graft failures following peripheral bypass procedures or coronary vein grafting.[1] Careful histological evaluation of failed infrainguinal grafts revealed the focal nature of the disease.[2,3] Three particular zones at the distal anastomosis, where the IH eventually develops, were identified. These areas are located at the toe and the heel near the suture line but also on the floor of the artery. The discussion of the causes and the factors contributing to their development comprise several biomechanical and immunological theories.[1] Among the favorite hypotheses are the concepts of compliance mismatch between PTFE graft and host artery and the arterial injury due to surgical reconstruction of the anastomosis.[4–7] However, these hypotheses could explain merely two of the three zones of IH formation, since the bed is not subjected to these traumas.

The compliance mismatch contributes only to stress fields in the vicinity of the anastomosis ring but not at the floor of the artery, while the arterial injury is equally restricted to the site of the arteriotomy and not involving the bed, which remains surgically untouched. Among the more accepted hypotheses is the concept of arterial wall adaptation to low wall shear stress, which leads to arterial remodeling. The low shear stress fields develop in areas of flow separation and stagnation, depending on the geometry of the anastomosis.[8–11]

Numerous studies investigated the local hemodynamics of end-side anastomoses using different methods for flow visualization and velocity measurements.[12–15] Shear stresses were estimated either by extrapolating measured point velocities, by use of the least-squares method or the Hagen–Poiseille law.[16–18] These methods however apply only for steady laminar flow and are very imprecise since shear rate is not obtained in a truly direct fashion.[19,20] The use of particle image velocimetry (PIV) allows a precise and

*Corresponding author. M. Heise, Charité, Campus Virchow Klinikum, Department of General, Transplantation and Vascular Surgery, Augustenburger Platz 1, 13353 Berlin, Germany.

1078–5884/000357 + 10 $35.00/0

instantaneous high resolution velocity measurement.[21,22] The obtained velocity vectors not only allow direct calculation of shear rates and stresses, a variety of additional fluid-dynamic parameters could additionally be derived.

The aim of the present study was to map the complex pulsatile flow fields inside a typical end-to-side anastomosis and to assess the fluid-dynamical environment in order to identify and quantify areas prone to development of IH. By characterizing the situation at the start and end-points of the supposed IH zones by measuring shear forces in terms of shear rates/stresses and vorticity, new insights into the pathophysiology of intimal hyperplasia could be drawn.

A silastic model of an end-side-anastomosis was used, incorporated into a mock circulation, which was driven by a Berlin heart. The flow was visualized by means of PIV, being the first technique to offer information about complete instantaneous velocity vector fields. Using the high resolution velocity information, additional flow dynamical features such as shear stress, strain rates and vorticity (rotation in z-direction) could be calculated and related to the known IH formation zones.

Material and Methods

Model

A silastic model of a funnel shaped distal femorocrural end-to-side anastomosis was fabricated.[23] The arterial diameter was 2.5 mm and the graft diameter 6 mm. The graft inlet angle was 140°. The mock circulation loop (Fig. 1) comprised a pneumatic artificial heart (Berlin Heart, Berlin, Germany), which was attached to a circuit of silastic tubes (internal diameter 1 cm, Rsch, Kernen, Germany). The flow rate was measured by means of an ultrasound flow meter (T206, Transonic Systems, Ithaca, U.S.A.), and the pressure by using a standard Statham transducer element (Transpac IV, Abbott Laboratories, Morgan Hill, U.S.A.). Peripheral resistance was modeled by means of small silastic suction tubes (Maersk Medical, Denmark), which were connected to the proximal and distal outflow section of the anastomosis model. A flow split of 1:1 was used. The length of the suction tubes (25 cm, internal diameter l2 Ch.) was adjusted to provide a resulting peripheral resistance of 0.5 mmHg/ml min peripheral resistance units (PRU) and a phase shift (hydraulic impedance) of −12°, which resemble real life values.[24,25]

The PIV measurements were taken at mean flow rates of 180 ml/min, which corresponds to a mean Reynolds number of 226 ($\mathrm{Re} = d{\cdot}u/\nu$; d = diameter, u = mean velocity, ν = kinematic viscosity). Applying this flow rate a mean pressure of 76 mmHg resulted at the level of the model inlet. The input and characteristic impedances were 0.4 and 0.22 mmHg/ml min (PRU) with a phase shift of −12°.

A mixture of approximately 58% water and 42% glycerin (Merck, Darmstadt, Germany) was used to obtain a viscosity in the range of blood. The viscosity was measured by means of a capillarimeter (Cavis, Raczek, Wedemark, Germany) and was adjusted to 4 mPa/s. Hollow glass spheres with a mean size of 9–13 μm (Sphericel, Potters Industries, Parsippany, U.S.A.) were used as tracer particles and seeded into the fluid. A temperature of 25 °C was maintained by a circulating heating pump, which additionally provided uniform distribution of the glass spheres.

Particle Image Velocimetry

High-speed digital PIV is an optical measurement technique that allows the acquisition of entire flow fields in a planar cross-section of a flow.[22] In contrast to laser doppler anemometry/velocimetry or duplex sonography, which only provide the velocity measurement of selected points within a flow field, the PIV technique allows to record large parts of a flow field instantaneously. This is a unique feature of this new technique. The seeded glass spheres were illuminated by means of a thin laser light sheet, which was directed into the centerline of the fluid flow.

A pulsed Nd:Yag laser (Minilite, Continuum, Santa Clara, U.S.A.) with an energy of 50 mJ at a repetition rate of 9 Hz was used for the illumination. The motion of the particles was recorded twice by means of a CCD-Camera (Flowmaster II, Lavison, Göttingen, Germany), using a time delay between the laser pulses of 200 μs and a resolution of 640 × 480 pixels. The flow meter signal was used to trigger the laser timing unit to the beginning of systole. Images were obtained at respective l00 ms steps beginning 50 ms after the onset of systole. Therefore, by applying a heart rate of 60 min^{-1} 10 sequential PIV recordings per heart period were obtained. For each time step five measurements were averaged. Using a systolic duration of 45%, systole ended after 450 ms.

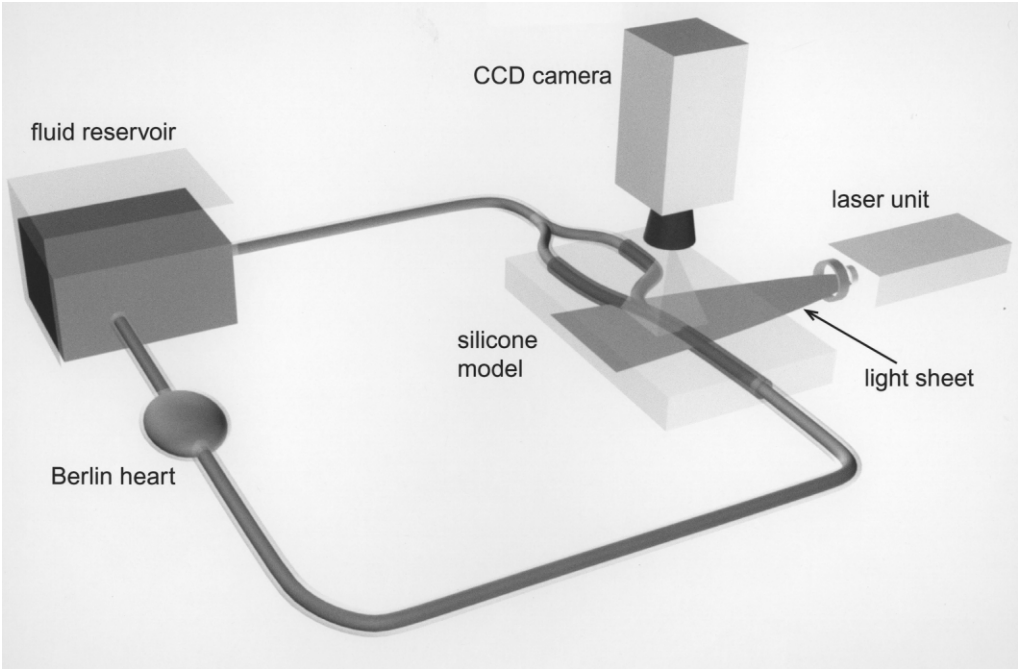

Fig. 1. Diagram of the mock circulation and PIV setup. The laser light is focused into a thin sheet of light which illuminates the fluid passing through the silicone model. The laser unit is triggered by the flowmeter signal and a Berlin heart is used to produce pulsatile flow.

Postprocessing of the Data

Image processing

The displacement of the particles between the two exposures is directly proportional to the local fluid velocity. The images were subsequently processed to extract the magnitude and direction of the particles in the flow. For evaluation the image was divided in small interrogation areas and the local displacement vector for the respective areas was determined by means of cross-correlation between two sequential images. The final interrogation cell size was 32×32 pixels. This technique provided a spatial resolution with a total of 1200 velocity vectors for an area of 10×15 mm^2. The entire anastomosis as well as the inflow and outflow regions were mapped and reconstructed (Fig. 2). For comparison of mean velocities rectangular areas encompassing 40–50 vectors were selected.

Data processing

The velocity field obtained by PIV can be used to estimate other fluid mechanically relevant quantities than velocity by means of differentiation or integration:

$$\text{Vorticity} = \omega_z = \frac{\partial V_y}{\partial x} - \frac{\partial V_x}{\partial y} \quad (1)$$

$$\text{Strain}_{(x)} = e_{(x)} = \frac{\partial V_x}{\partial x} \quad (2)$$

$$\text{Shear rate} = h = \frac{\partial V_y}{\partial x} + \frac{\partial V_x}{\partial y} \quad (3)$$

$$\text{Shear stress} = \tau = \nu\frac{\partial V_y}{\partial x} + \frac{\partial V_x}{\partial y}. \quad (4)$$

The vector data were used to calculate vorticity ω (Equation (1)), strain rates in x-direction e_x (Equation (2)) and shear rates h (Equation (3)) using the partial derivatives of the velocity components ($\partial V_{x,y}$) to both x and y. Application of Equation (4) allowed computation and three-dimensional visualization (Fig. 5) of shear stresses τ. Of the differential quantities, the vorticity field is of special interest because this quantity can be more useful in the study of flow phenomena than the velocity field by itself, especially in highly complex vortical flows. Vorticity (ω_z) computes the z-component of the rotation-vector of the fluid and therefore indicates high shear areas (Fig. 2).[26] ω_z is positive, if the flow field is turning clockwise and negative, if the flow field is turning counterclockwise.

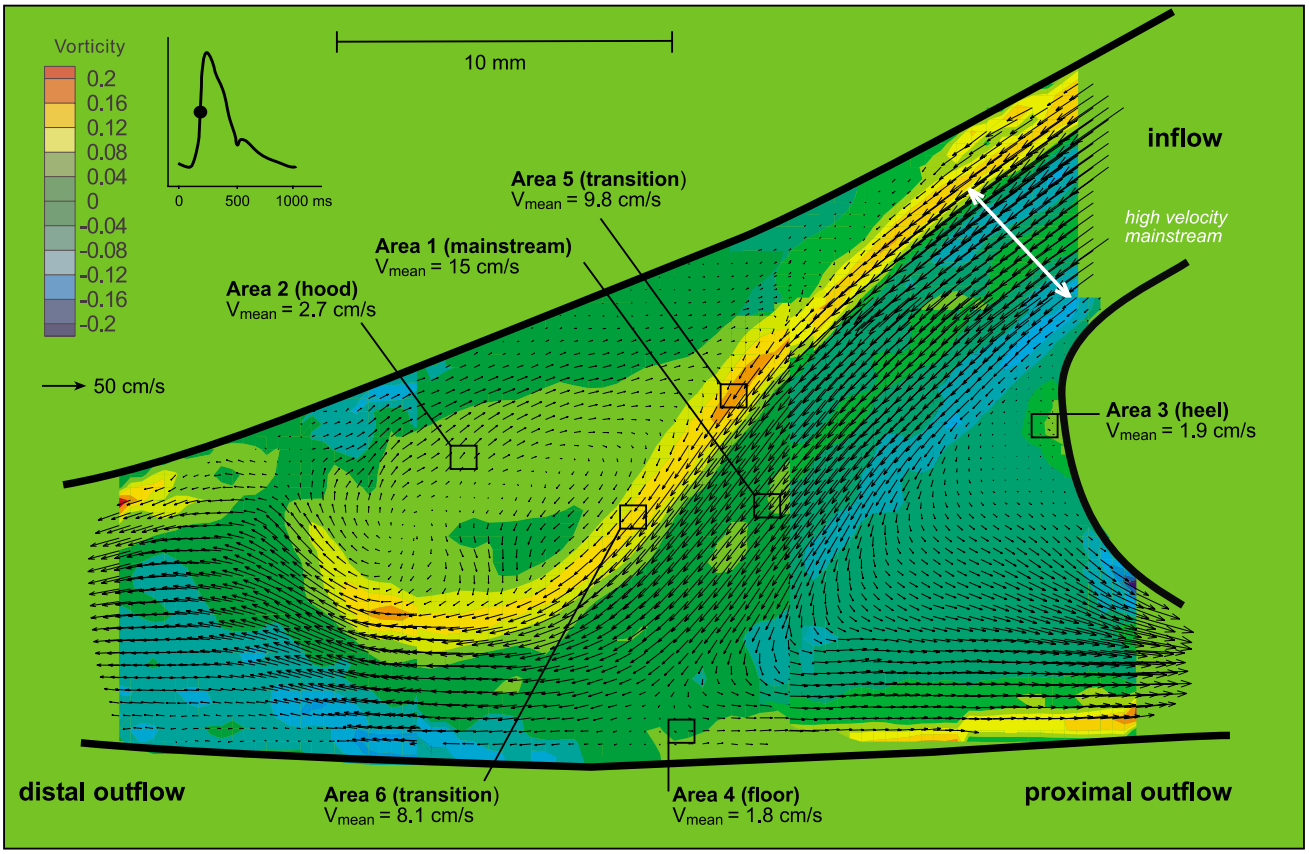

Fig. 2. Mapping of the end-side anastomosis by means of four PIV measurements at 250 ms. A high velocity mainstream is entering the anastomosis centre and diverting towards the proximal and distal outflow. The large toe and heel separations have been developed. Velocities in the separation fields are significantly lower than in the effective mainstream. The arrows are depicting velocity vectors, with the length proportional to velocity. Colours represent vorticity ω_z (rotation in z-direction). The high vorticity fields indicate high shear forces in the transition zones between mainstream and separations.

Statistics

Data are expressed as mean ± standard deviation. A Student *t*-test was used to compare velocities, shear stresses and strain rates in the mainstream and separation fields. *p*-values <0.05 were considered statistically significant.

Results

The flow pattern inside the anastomosis comprised a high velocity mainstream (A; area 1 in Figs 2 and 3) with two separation areas (B, C; areas 2 and 3 in Fig. 2), located at the anastomosis ring and one stagnation zone (D; area 4 in Fig. 2) at the floor of the artery.

High velocity mainstream

The mainstream entered the anastomosis area with velocities ranging from 26 to 286 cm/s (mean 150 ± 93 cm/s, Fig. 2). Mean shear stresses and strain rates are outlined in Table 1. The velocity profile at the entrance level was nearly parabolic, as expected in fully developed pipe flow (Fig. 4). During the transit through the centre of the anastomosis, the velocity profile changed with a marked decrease of the mainstream's central velocities, which led to a marked attenuation of the velocity profile (Fig. 4). This corresponded to an energy loss and was attributed to the simultaneous development of the separation and stagnation zones at the lateral parts of the mainstream.

At the lower part of the anastomosis centre the mainstream divided towards the distal and proximal outlets. Distally, the mainstream entered the outlet with a characteristic deflection towards the hood region. This deflection corresponded to the characteristic configuration of the intimal hyperplasia at the toe, as depicted by Bassiouny and others (Fig. 3).[2,27]

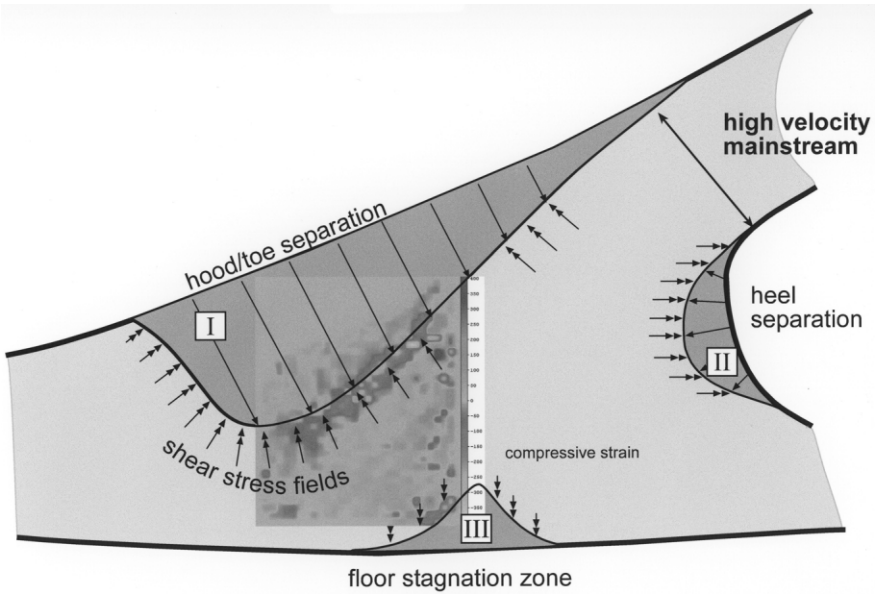

Fig. 3. Diagram of the three known locations (I–III) of intimal hyperplasia development in an end-side anastomosis. We hypothesized that the hyperplasia of fibroblasts continues (→) until the high shear stress fields (↠) of the transition zones depicted in Figure 2 are reached. In these areas compressive strain fields were additionally found (plot inserted). The extent of IH formation depends on the width of the high velocity mainstream (= effective mainstream).

Hood/toe separation zone

The flow separation from the high velocity mainstream started at the inflow region when the wall diverged and the wall–mainstream angle increased over 6°, which is a typical property of flow in a pipe.[26] A large separation zone (maximal diameter 6×14 mm) was formed, occupying a significant part (about 60%) of the central anastomosis cross-section. Due to the extent of the separation and the size mismatch between the anastomosis centre and the distal outlet, a backward flow was formed, which partly impinged on the mainstream in a normal direction and partly embraced the mainstream laterally. The vortex, which turned in a clockwise direction, was formed 50 ms after the outset of the systole and lasted through the entire cardiac cycle. The velocities inside the separation zone ranged between 11 and 56 cm/s (mean 27 ± 17 cm/s), and differed by statistical significance with respect to the mainstream ($p < 0.001$). The shear stresses were from 0.12 to 1 dynes/cm^2 (mean 0.35 ± 0.2 dynes^2, $p < 0.05$). Therefore, in the entire hood/toe separation zone shear stresses were observed, which were significantly lower than average arterial wall shear stress levels and significantly lower than the mainstream velocities and shear rates/stresses, respectively. Between the high velocity mainstream and the medial part of the hood vortex a transition zone was identified (areas 5 and 6 in Fig. 2), which had remarkable fluid-dynamical features providing a potential link to the development of intimal hyperplasia. In this zone, high shear stresses (range 0.16–2 dynes/cm^2, mean 1 ± 0.7 dynes/cm^2) and vorticity rates existed, which resulted from the friction of the lateral mainstream with the retrograde flowing vortex (Fig. 5). In this particular area, high negative strain rates (range −4 to −105 s^{-1}, mean −43 ± 12 s^{-1}) in a direction against the separation zone were found. Since negative strain rates correspond to compressive strain, a significant compressive force existed inside the flow field, which pressed against the low shear separation area.[26] Therefore, at least two forces acting against the zone were detectable, forming a fluid dynamical "barrier" within the flow field.

Table 1. Comparison of mean velocities, shear stress and strain rates e_x in selected areas of the distal end-to-side anastomosis as depicted in Figure 2. (Values are mean ± standard deviation).

Variable	Area 1 (mainstream)	Area 2 (hood)	Area 3 (heel)	Area 4 (floor)	Area 5 (transition)	Area 6 (transition)
Velocity (cm/s)	150 ± 93	27 ± 17	19 ± 10	18 ± 9	10 ± 1	8 ± 1
Shear stress (dynes/cm^2)	0.72 ± 0.4	0.35 ± 0.2	0.28 ± 0.1	0.45 ± 0.2	0.98 ± 0.7	1 ± 0.7
Strain rates, $e_{x'}$ (s^{-1})	10 ± 3	−3 ± 2	1 ± 1	14 ± 2	−43 ± 12	−30 ± 7

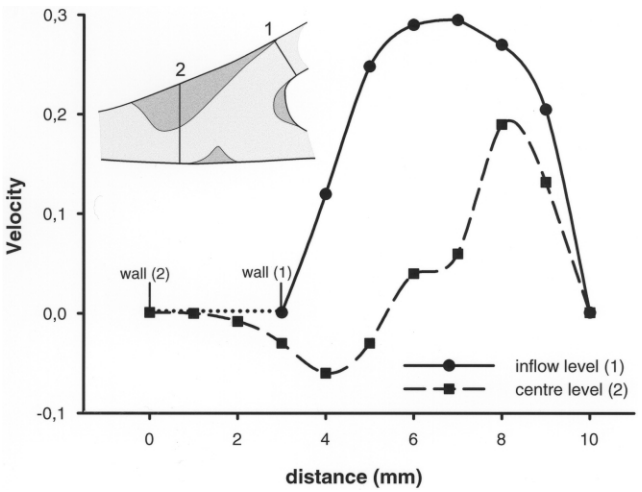

Fig. 4. Comparison of velocity profiles at the model inflow level (1) and the anastomosis centre (2). The expansion of the anastomosis leads to an attenuation of the velocity profile and corresponded to a loss of kinetic energy.

Heel separation zone

The heel separation zone equally developed immediately after the beginning of the systole. The separation occurred, like in the hood separation case, as the mainstream/wall angle increased over 6°. The vortex was turning counterclockwise with shear stresses ranging from 0.11 to 0.52 dynes/cm^2, mean 0.28 ± 0.1 dynes/cm^{-2}). The velocities ranged from 8 to 57 cm/s (mean 19 ± 10 cm/s). Compared to the hood separation, the heel zone was somewhat smaller with a maximal diameter of 6 × 4 mm.

Floor stagnation zone

On the floor of the artery, a small triangular shaped stagnation zone developed at 250 ms (Fig. 2). The flow stagnation occurred when the mainstream flow divided into the proximal and distal outflow. The stagnation streamline corresponded to the central portion of the mainstream. The velocities measured in this area were 8–40 cm/s (mean 18 ± 9 cm/s) and shear stresses, which ranged from 0.22 to 0.94 dynes/cm^2 (mean 0.45 ± 0.1 dynes/cm^2, Table 1).

Discussion

The development of anastomotical IH represents one of the major causes for both PTFE and vein graft failures in the long term.[1,27,28] The discussion of the pathophysiology of intimal hyperplasia comprises several theories, which more or less contribute to the current knowledge of the IH development.[2,29,30] However, the research is demanding since the IH formation is a chronic process and direct visualization, i.e., by means of measuring high resolution velocity fields is not available *in vivo*. Without the two-dimensional velocity information quantitative data regarding shear stresses or vorticity are not directly accessible and therefore have to be computed or otherwise estimated.[14,19] Conventional Laser Doppler Velocimetry/Anemometry (LDV) or duplex sonography merely permit velocity measurements of single points within the flow field.

The main advantage of the new PIV technique compared to other methods for measuring flow velocity is, that the whole flow field within the plane of the light sheet is recorded instantaneously. Therefore the PIV technique is best suited for the measurement of unsteady flow fields.[22] Postprocessing of the velocity data yields several fluid dynamical important variables, like shear stresses, strain rates and vorticity. The latter is a measure for rotation of the fluid in *z*-direction, thereby indicating high shear fields.[26]

The local hemodynamics of end-side anastomoses have been addressed in a number of studies, using a variety of methods for flow visualization.[12–15] A recent study first used PIV for this purpose and the overall results in terms of localization of separation zones were comparable.[21] Several studies additionally attempted to calculate shear rates and stresses, particularly near the wall, since wall shear stresses are believed to correlate with IH formation.[16,20,31] The previous studies used different approaches to evaluate the wall shear rate. The first was to measure the shear rate exactly with electrochemical or hot-film probes.[32] However, these measurements are accurate only with steady flow.[19] A second method calculates shear rates using the velocity profile measured at desired sites by means of LDV and the third approach derived wall shear rate from the Hagen–Poiseuille law, which assumes steady laminar flow and therefore could not be used for the disturbed velocity profile inside an end-side anastomosis due to large separation zones, as shown in Fig. 4.[33–36] By using PIV, we were able to obtain shear rates not only directly at the wall but throughout the entire flow field in a high resolution for every desired time step.

We investigated the spatial hemodynamics at the distal anastomosis of peripheral bypasses in a silastic model, using pulsatile flow, produced by an artificial heart, and blood like viscosity at 25°. The distal runoff was adjusted to human arterial values with consideration of both steady and pulsatile resistances. The silastic model resembles the elastic behavior of human arteries more than glass models.

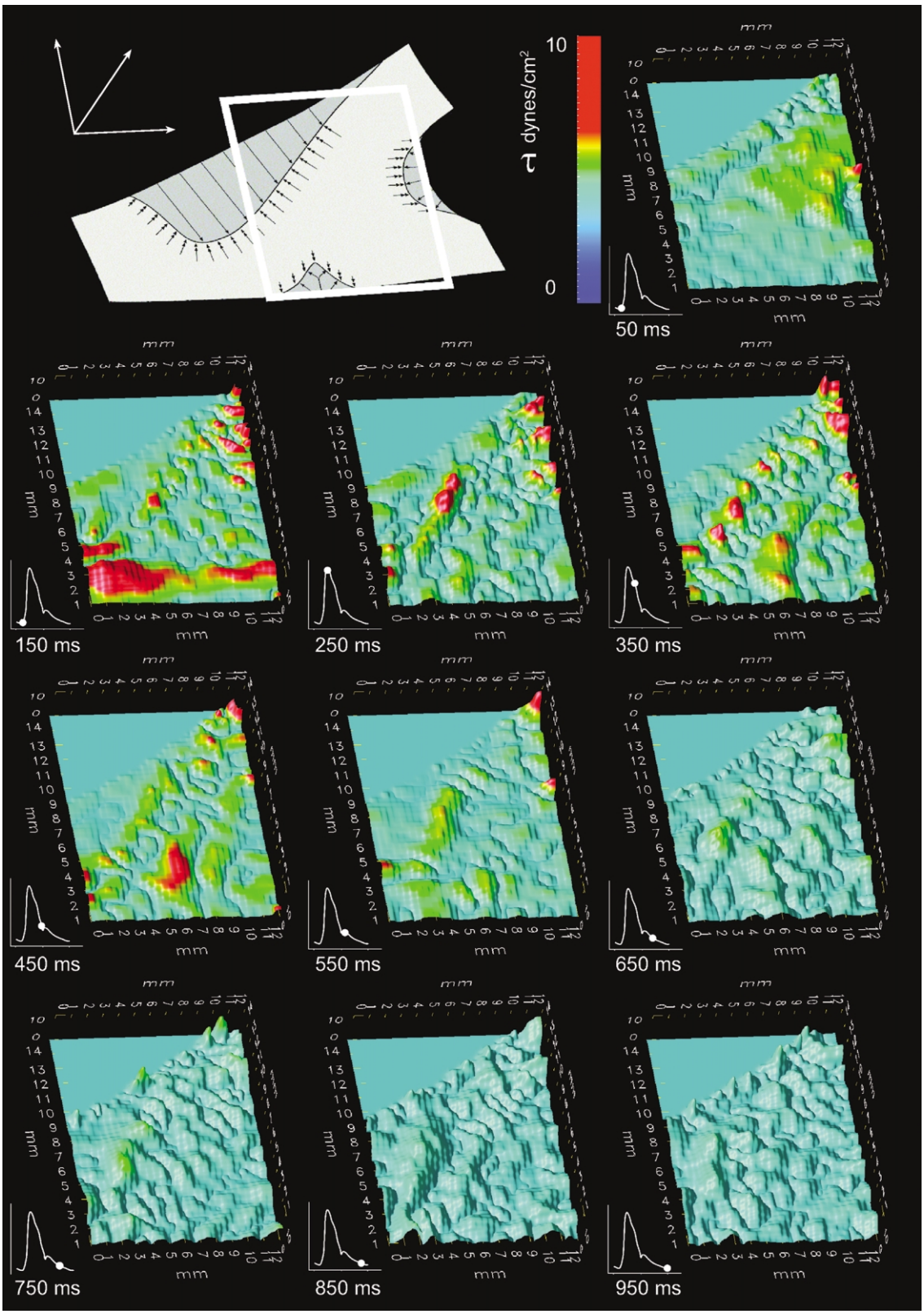

Fig. 5. Diagram of shear stress progression at the anastomosis centre during the cardiac cycle. Between 250 and 550 ms high shear stresses develop at the transition zone between mainstream and separation areas. During the entire cardiac cycle the shear stresses within the separation zones were significantly lower than arterial wall shear stresses.

The flow visualization revealed that a high velocity mainstream with fully developed laminar flow entered the anastomosis area. When the walls of the anastomosis diverged and the mainstream to wall angle increased over 6°, two boundary layers with lower velocities were formed between the mainstream and the diverging section of the anastomosis. As the angle between the wall and the mainstream increased further and the mainstream proceeded towards the centre of the anastomosis, a large vortex with a significant backward flow resulted at the hood area, which eventually re-entered the mainstream at the entrance region of the anastomosis.

At the heel of the anastomosis a similar but smaller separation field was found, which equally developed after the mainstream–wall angle diverged. Here, a small counterclockwise flowing vortex resulted with somewhat higher shear stresses than the hood vortex, particularly near the wall. Finally, a stagnation zone developed on the floor of the anastomosis due to the diversion of the mainstream into the proximal and distal outflow.

The most important findings compared to previous studies, were fluid-dynamically remarkable areas at the transition between the three low shear zones and the mainstream. In this particular region high shear zones existed during the entire cardiac cycle, as indicated by high vorticity fields and high shear stresses (Figs 4 and 5). In addition negative strain rates, denoting compressive forces, were present along the mainstream–separation interface. It was previously not known that such transition zones existed between mainstream and separations in the flow field. The existence of these zones explains the focal nature of intimal hyperplasia development, since they hypothetically possess the force to limit the IH formation to the separation zones.

Comparison of the location of the separation and stagnation zones with the three zones of IH development formerly identified by Bassiouny and others, revealed a remarkable analogy, they were in fact congruent.[2,3,37] It therefore appears that the IH forms in all sections of the anastomosis were the velocities and shear rates were substantially lower than in the high velocity effective mainstream. Therefore this study supports the low-shear theory which was introduced by several authors and was recently supported by Meyerson *et al*., who were able to clearly demonstrate the relation between extremely low shear and IH formation.[8–11,38] It is therefore useful to investigate the fluid-dynamical environment of the start and endpoints of the IH development at the wall and the vortex-mainstream interface. Among the more accepted hypotheses is the concept of arterial wall adaptation to low wall shear stress, which leads to arterial remodeling.[36,39–41] The histological examination of the IH lesions showed that the hyperplasia was not a simple thickening of the endothel but rather an active process, in terms of hyperplasia of subendothelial smooth muscle cells.[3,39] These proliferated, supposedly triggered by low wall shear stress. Several studies have proposed at least four types of mechanoreceptors, that are able to transduce signals via endothel cells in response to shear stress.[39,42,43] This is particularly useful during the growth in order to fit the arterial diameter to the increased blood supply of growing tissue. The diameter increases until the normal wall shear stress relation is re-established.[41] On the other hand, lower shear stresses lead to arterial remodeling in terms of myointimal hyperplasia.[8,10] We hypothesized that the fibroblasts growth continues "undisturbed" until the high shear stress zones, as indicated by high vorticity rates along the separation fields and the effective mainstream, are reached and the wall diversion angle leading to flow separation reduced. In this particular area, negative strain rates in direction against the separations were found, which correspond to compressive strain. Hence, in these transition areas both compressive and shear forces are acting on the separation/stagnation zone borders. These forces supposedly provide the power to discontinue the further progression of the fibroblasts growth. We hypothesized that they induce the stop signal via the endothelial pathway to the subendothelial fibroblasts. In the high shear fields in the central region of the anastomosis conditions were found, which resemble the conditions at the wall in fully developed laminar flow. We therefore concluded that the relation between the effective, high momentum mainstream and the low shear separation/stagnation zones is responsible for the extent of the IH development. Simply stated, the broader the effective mainstream, the smaller the resulting IH zones and vice versa. Application of this theory explains the heterogeneous IH formation in various clinical and experimental conditions. As indicated by Meyerson, the IH formation in their study was limited to a small area, and was smaller than expected, which was confirmed by other studies.[10,38,44] However, most experimental models dealing with IH use carotidal models with insertion of venous patches or interposition of whole veins.[35,38,44–46] By assuming a broad effective mainstream due to the low resistance which is associated with carotidal runoff, small separation zones had to be anticipated. In addition the hemodynamic forces acting on the anastomosis are amplified in peripheral settings due to increased impedance

values, which could be neglected in cerebral runoff.[24, 25]

Summarized, the development of fibromuscular hyperplasia connotes a physiological adoption of the arterial wall to lowered shear stresses prevailing in areas of flow separation. The IH layer growth until the high shear transition zone between the effective mainstream and the separation/stagnation zones is reached. Flow separation occurs at a wall diversion angle greater than 6°. Hence, the development of intimal hyperplasia is predictable, once the exact velocities and shear rates/stresses are known. The measurement of whole field velocities is currently restricted to *in vitro* methods, like the PIV. A major disadvantage of PIV represents the fact that in the current setting measurements were obtained in a two-dimensional plane. Therefore, three-dimensional information is still limited. In future studies the various types of distal anastomoses should be investigated with regard to their fluid-dynamical behaviour to find the most advantageous form. By considering principles of fluid-dynamics in future anastomoses design, IH development could be reduced.

Acknowledgements

This study was supported in part by the Else Kröner-Fresenius-Stiftung, Bad Homburg, Germany.

References

1 Lemson MS, Tordoir JH, Daemen MJ, Kitslaar PJ. Intimal hyperplasia in vascular grafts. *Eur J Vasc Endovasc Surg* 2000; **19**: 336–350.
2 Bassiouny HS, White S, Glagov S, Choi E, Giodens DP, Zarins CK. Anastomotic intimal hyperplasia: mechanical injury or flow induced. *J Vasc Surg* 1992; **15**: 708–716.
3 Sottiurai VS, Yao JS, Flinn WR, Batson RC. Intimal hyperplasia and neointima: An ultrastructural analysis of thrombosed grafts in humans. *Surgery* 1983; **93**: 809–817.
4 Trubel W, Schima H, Moritz A *et al.* Compliance mismatch and formation of distal anastomotic intimal hyperplasia in externally stiffened and lumen-adapted venous grafts. *Eur J Vasc Endovasc Surg* 1995; **10**: 415–423.
5 Abbott WM, Megerman J, Hasson JE, L'Italien G, Warnock DF. Effect of compliance mismatch on vascular graft patency. *J Vasc Surg* 1987; **5**: 376–382.
6 Ballyk PD, Walsh C, Butany J, Ojha M. Compliance mismatch may promote graft-artery intimal hyperplasia by altering suture-line stresses. *J Biomech* 1998; **31**: 229–237.
7 Clowes AW, Clowes MM, Fingerle J, Reidy MA. Regulation of smooth muscle cell growth in injured artery. *J Cardiovasc Pharmacol* 1989; **14**(Suppl 6): S12–S15.
8 Morinaga K, Okadome K, Kuroki M, Miyazaki T, Muto Y, Inokuchi K. Effect of wall shear stress on intimal thickening of arterially transplanted autogenous veins in dogs. *J Vasc Surg* 1985; **2**: 430–433.
9 Gnasso A, Carallo C, Irace C *et al.* Association between intima-media thickness and wall shear stress in common carotid arteries in healthy male subjects. *Circulation* 1996; **94**: 3257–3262.
10 Meyerson SL, Skelly CL, Curi MA *et al.* The effects of extremely low shear stress on cellular proliferation and neointimal thickening in the failing bypass graft. *J Vasc Surg* 2001; **34**: 90–97.
11 Kohler TR, Kirkman TR, Kraiss LW, Zierler BK, Clowes AW. Increased blood flow inhibits neointimal hyperplasia in endothelialized vascular grafts. *Circ Res* 1991; **69**: 1557–1565.
12 Ojha M, Cobbold RS, Johnston KW. Hemodynamics of a side-to-end proximal arterial anastomosis model. *J Vasc Surg* 1993; **17**: 646–655.
13 Ojha M, Ethier CR, Johnston KW, Cobbold RS. Steady and pulsatile flow fields in an end-to-side arterial anastomosis model. *J Vasc Surg* 1990; **12**: 747–753.
14 Noori N, Scherer R, Perktold K *et al.* Blood flow in distal end-to-side anastomoses with PTFE and a venous patch: results of an *in vitro* flow visualisation study. *Eur J Vasc Endovasc Surg* 1999; **18**: 191–200.
15 Rowe CS, Carpenter TK, How TV, Harris PL. Local haemodynamics of arterial bypass graft anastomoses. *Proc Inst Mech Eng* 1999; **213**: 401–409.
16 Ojha M. Wall shear stress temporal gradient and anastomotic intimal hyperplasia. *Circ Res* 1994; **74**: 1227–1231.
17 Lei M, Archie JP, Kleinstreuer C. Computational design of a bypass graft that minimizes wall shear stress gradients in the region of the distal anastomosis. *J Vasc Surg* 1997; **25**: 637–646.
18 Ling SC, Atabek HB, Letzing WG, Patel DJ. Nonlinear analysis of aortic flow in living dogs. *Circ Res* 1973; **33**: 198–212.
19 Lou Z, Yang WJ, Stein PD. Errors in the estimation of arterial wall shear rates that result from curve fitting of velocity profiles. *J Biomech* 1993; **26**: 383–390.
20 Ojha M. Spatial and temporal variations of wall shear stress within an end-to-side arterial anastomosis model. *J Biomech* 1993; **26**: 1377–1388.
21 Bates CJ, O'Doherty DM, Williams D. Flow instabilities in a graft anastomosis: a study of the instantaneous velocity fields. *Proc Inst Mech Eng* 2001; **215**: 579–587.
22 Raffel M, Willert C, Kompenhans J. *Particle Image Velocimetry.* Berlin: Springer, 1998.
23 Krüger U. *Hämodynamische Optimierung von Gefäßprothesen*. Berlin: Verlag Dr Köster, 1998.
24 Heise M, Kruger U, Settmacher U, Sklenar S, Neuhaus P, Scholz H. A new method of intraoperative hydraulic impedance measurement provides valuable prognostic information about infrainguinal graft patency. *J Vasc Surg* 1999; **30**: 301–308.
25 Klanchar M, Tarbell JM, Wang DM. *In vitro* study of the influence of radial wall motion on wall shear stress in an elastic tube model of the aorta. *Circ Res* 1990; **66**: 1624–1635.
26 Smits AJ. *A Physical Introduction to Fluid Mechanics*. New York: Wiley, 1999.
27 Ojha M, Leask RL, Johnston KW, David TE, Butany J. Histology and morphology of 59 internal thoracic artery grafts and their distal anastomoses. *Ann Thorac Surg* 2000; **70**: 1338–1344.
28 Imparato AM, Bracco A, Kim GE, Zeff R. Intimal and neointimal fibrous proliferation causing failure of arterial reconstructions. *Surgery* 1972; **72**: 1007–1017.
29 Dobrin PB, Littooy FN, Endean ED. Mechanical factors predisposing to intimal hyperplasia and medial thickening in autogenous vein grafts. *Surgery* 1989; **105**: 393–400.
30 Greenwald SE, Berry CL. Improving vascular grafts: the importance of mechanical and haemodynamic properties. *J Pathol* 2000; **190**: 292–299.
31 Keynton RS, Evancho MM, Sims RL, Rittgers SE. The effect of graft caliber upon wall shear within *in vivo* distal vascular anastomoses. *J Biomech Eng* 1999; **121**: 79–88.
32 Ling SC, Atabek HB, Fry DL, Patel DJ, Janicki JS. Application of heated-film velocity and shear probes to hemodynamic studies. *Circ Res* 1968; **23**: 789–801.
33 Deters OJ, Bargeron CB, Mark FF, Friedman MH. Measurement of wall motion and wall shear in a compliant arterial cast. *J Biomech Eng* 1986; **108**: 355–358.

34 Friedman MH, Deters OJ. Correlation among shear rate measures in vascular flows. *J Biomech Eng* 1987; **109**: 25–26.
35 Binns RL, Ku DN, Stewart MT, Ansley JP, Coyle KA. Optimal graft diameter: effect of wall shear stress on vascular healing. *J Vasc Surg* 1989; **10**: 326–337.
36 Zarins CK, Zatina MA, Giddens DP, Ku DN, Glagov S. Shear stress regulation of artery lumen diameter in experimental atherogenesis. *J Vasc Surg* 1987; **5**: 413–420.
37 Fillinger MF, Reinitz ER, Schwartz RA *et al.* Graft geometry and venous intimal-medial hyperplasia in arteriovenous loop grafts. *J Vasc Surg* 1990; **11**: 556–566.
38 Berguer R, Higgins RF, Reddy DJ. Intimal hyperplasia. An experimental study. *Arch Surg* 1980; **115**: 332–335.
39 Traub O, Berk BC. Laminar shear stress: mechanisms by which endothelial cells transduce an atheroprotective force. *Arterioscler Thromb Vasc Biol* 1998; **18**: 677–685.
40 Gibbons GH, Dzau VJ. The emerging concept of vascular remodeling. *N Engl J Med* 1994; **330**: 1431–1438.
41 Kamiya A, Togawa T. Adaptive regulation of wall shear stress to flow change in the canine carotid artery. *Am J Physiol* 1980; **239**: H14–H21.
42 Davies PF. Flow-mediated endothelial mechanotransduction. *Physiol Rev* 1995; **75**: 519–560.
43 Fisher AB, Al Mehdi AB, Manevich Y. Shear stress and endothelial cell activation. *Crit Care Med* 2002; **30**: S192–S197.
44 Suggs WD, Henriques HF, Depalma RG. Vein cuff interposition prevents juxta-anastomotic neointimal hyperplasia. *Ann Surg* 1988; **207**: 717–723.
45 Jackson ZS, Ishibashi H, Gotlieb AI, Langille BL. Effects of anastomotic angle on vascular tissue responses at end-to-side arterial grafts. *J Vasc Surg* 2001; **34**: 300–307.
46 Zwolak RM, Adams MC, Clowes AW. Kinetics of vein graft hyperplasia: association with tangential stress. *J Vasc Surg* 1987; **5**: 126–136.

Accepted 25 October 2002